

Supporting information

Observing a Model Ion Channel Gating Action in Model Cell Membranes in Real Time *in Situ*: Membrane Potential Change Induced Alamethicin Orientation Change

Shuji Ye,^{1*} Hongchun Li,¹ Feng Wei,¹ Joshua Jasensky,² Andrew P. Boughton,³ Pei Yang,³
Zhan Chen^{2,3*}

¹Hefei National Laboratory for Physical Sciences at Microscale and Department of
Chemical Physics, University of Science and Technology of China, Hefei, Anhui,
P.R.China 230026

²Department of Biophysics and ³Department of Chemistry, University of Michigan, Ann
Arbor, MI 48109, USA

1. Polarized ATR-FTIR experiments

A Nicolet Magna-IR 550 spectrometer was used to collect attenuated total reflectance-Fourier transform infrared (ATR-FTIR) spectra with a standard 45 °ZnSe ATR cell and a ZnSe grating polarizer (from Optometrics LLC). The ZnSe crystal (Specac Ltd. Woodstock, GA) was cleaned using the same procedures used for CaF₂ prisms. Lipid bilayers were deposited onto the ZnSe crystal surface using the LB/LS method mentioned in the article. All lipid bilayers (in contact with water) were flushed with D₂O multiple times to avoid signal confusion between the O-H bending mode and the peptide amide I mode and to ensure a better S/N ratio in the peptide amide I band frequency region. After an equilibration period of 2 hours, a polarized background spectrum of the lipid bilayer/D₂O interface was recorded. A 15 μL alamethicin solution (in methanol with a concentration of 2.5 mg/mL) was injected into a 1.6 mL reservoir and given 1 hour to allow alamethicin adsorption to the bilayer to reach equilibrium before polarized SFG spectra were collected. Finally, the amide I signal of alamethicin was obtained by

subtracting the background spectrum of the bilayer/D₂O interface recorded earlier. All the spectra collected here were averages of 256 scans with a 2 cm⁻¹ resolution.

2 SFG experiments

The SFG experimental setup was similar to that described in our earlier publications.¹ In this research, all SFG experiments were carried out at the room temperature (25 °C). SFG spectra from interfacial alamethicin with different polarization combinations including ssp (s-polarized SF output, s-polarized visible input, and p-polarized infrared input) and ppp were collected using the near total internal reflection geometry.

3. Orientation angle of peptides deduced from ATR-FTIR

ATR-FTIR spectroscopy has been widely used to analyze peptide/protein secondary structures on surfaces or at interfaces and to determine the orientation of such secondary structures.² In ATR-FTIR studies, the tilt angle (θ) of the helices can be determined from the measured infrared linear dichroic ratio (R) in ATR-FTIR using p- and s-polarized IR beams:^{2,3}

$$R = \frac{A_{//}}{A_{\perp}} = \frac{E_z^2 k_z + E_x^2 k_x}{E_y^2 k_y} \quad (\text{S1})$$

where E_i (i=x,y,z) is the electric field amplitude of the evanescent wave at the surface of the internal reflection element, and k_i (i=x,y,z) is a component of the integrated absorption coefficient in the lab fixed coordinate system. E_i (i=x,y,z) depends on the incidence angle of the IR beam at the solid-liquid interface, and the refractive indices of the internal reflection element (ATR crystal), the thin film (bilayer), and the bulk contacting medium (D₂O). We calculated the value of E_i (i=x,y,z) using the formula published in the literature.^{2,3} If we model the orientation distribution of a helix in the lab-fixed coordinate

system as a Gaussian distribution ($f = \frac{1}{\sqrt{2\rho S}} e^{-\frac{(x-q)^2}{2S^2}}$), k_i (i=x,y,z) is given as follows:³

$$\langle k_x \rangle = \langle k_y \rangle = \frac{\cos(\vartheta)^2 \left(\frac{1}{2} - \frac{\cos(2q)}{2e^{2S^2}} \right)}{2} + \frac{\sin(\vartheta)^2}{4} + \frac{\sin(\vartheta)^2 \left(\frac{1}{2} + \frac{\cos(2q)}{2e^{2S^2}} \right)}{4} \quad (\text{S2})$$

$$\langle k_z \rangle = \cos(\alpha)^2 \left(\frac{1}{2} + \frac{\cos(2\theta)}{2e^{2\sigma^2}} \right) + \frac{\sin(\alpha)^2 \left(\frac{1}{2} - \frac{\cos(2\theta)}{2e^{2\sigma^2}} \right)}{2} \quad (\text{S3})$$

where θ and σ are the tilt angle between the helix's principal axis and the surface normal and the orientation distribution width respectively; α is the angle between the transition dipole moment and the principal axis of the helix, which equals to 38° for α -helix and 45° for 3_{10} helix.^{4,5} The bracket denotes the time and ensemble average. When $\sigma = 0$, the orientation distribution is a δ -distribution. Since ATR-FTIR only provides one experimentally measured parameter (R), based on equations S1 to S3, the tilt angle θ can be determined by knowing the value of E_i ($i=x,y,z$), and α , and assuming a certain value of σ . The relation between the intensity ratio (R) in the polarized ATR-FTIR measurement and the α -helix orientation is shown in Figure S1.

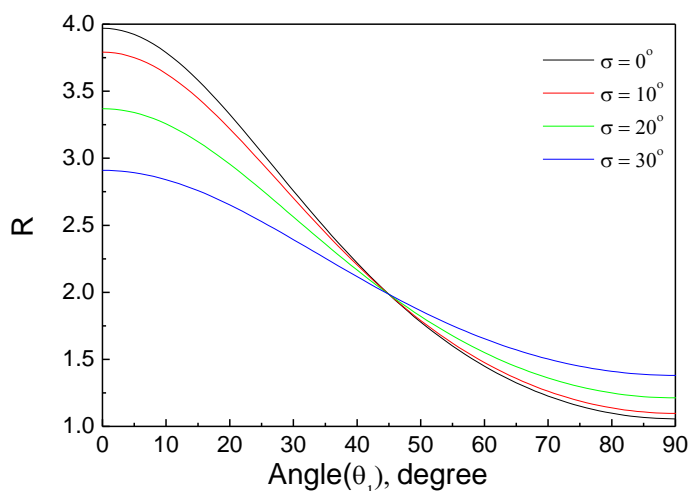


Figure S1. The relation between the intensity ratio (R) in the polarized ATR-FTIR measurement and the α -helix orientation.

4. Orientation angle of peptides deduced from SFG

The molecular orientation information can be obtained by relating SFG susceptibility tensor elements χ_{ijk} ($i, j, k = x, y, z$) to the SFG molecular hyperpolarizability tensor elements β_{lmn} ($l, m, n = a, b, c$).⁶ Our lab has developed a methodology to determine the orientation of α -helical structures using SFG amide I

spectra collected with different polarization combinations. This method has been introduced in our previous papers⁷⁻¹¹.

The components of $\chi_{eff}^{(2)}$ of ssp and ppp polarization combinations are given in equations (S4)-(S5) in the lab coordinate system which is defined as the z-axis being along the surface normal and the x-axis being in the incident plane.^{1, 6-11}

$$\chi_{eff,ssp}^{(2)} = L_{yy}(\omega_{SF})L_{yy}(\omega_{Vis})L_{zz}(\omega_{IR})\sin\beta_{IR}\chi_{yyz}^{(2)} \quad (S4)$$

$$\begin{aligned} \chi_{eff,ppp}^{(2)} = & -L_{xx}(\omega_{SF})L_{xx}(\omega_{Vis})L_{zz}(\omega_{IR})\cos\beta_{SF}\cos\beta_{Vis}\sin\beta_{IR}\chi_{xxz}^{(2)} \\ & -L_{xx}(\omega_{SF})L_{zz}(\omega_{Vis})L_{xx}(\omega_{IR})\cos\beta_{SF}\sin\beta_{Vis}\cos\beta_{IR}\chi_{xzx}^{(2)} \\ & +L_{zz}(\omega_{SF})L_{xx}(\omega_{Vis})L_{xx}(\omega_{IR})\sin\beta_{SF}\cos\beta_{Vis}\cos\beta_{IR}\chi_{zxx}^{(2)} \\ & +L_{zz}(\omega_{SF})L_{zz}(\omega_{Vis})L_{zz}(\omega_{IR})\sin\beta_{SF}\sin\beta_{Vis}\sin\beta_{IR}\chi_{zzz}^{(2)} \end{aligned} \quad (S5)$$

where β_{SF} , β_{Vis} and β_{IR} are the angles between the surface normal and the sum frequency beam, the input visible beam, and the input IR beam, respectively. L_{ii} ($i = x, y$ or z) denotes the Fresnel coefficients. Using the near total reflection geometry, the first three items in equation (S5) are approximated to be 0. Therefore the χ_{yyz} and χ_{zzz} susceptibility components are the main contributors to the ssp and ppp signals, respectively. With an azimuthal symmetry of the peptide molecules at the interface, the dependence of χ_{yyz} and χ_{zzz} susceptibility components on the molecular hyperpolarizability can be described by the following equations.⁶⁻¹²

For the A mode:

$$\chi_{A,xxz} = \chi_{A,yyz} = \frac{1}{2}N_s[(1+r)\langle\cos\theta\rangle - (1-r)\langle\cos^3\theta\rangle]\beta_{ccc} \quad (S6)$$

$$\chi_{A,zzz} = N_s[r\langle\cos\theta\rangle + (1-r)\langle\cos^3\theta\rangle]\beta_{ccc} \quad (S7)$$

For the E₁ mode:

$$\chi_{E1,xxz} = \chi_{E1,yyz} = -N_s(\langle\cos\theta\rangle - \langle\cos^3\theta\rangle)\beta_{aca} \quad (S8)$$

$$\chi_{E1,zzz} = 2N_s(\langle\cos\theta\rangle - \langle\cos^3\theta\rangle)\beta_{aca} \quad (S9)$$

where $r = \beta_{aad}/\beta_{ccc}$, and β_{aac} , β_{aca} and β_{ccc} are the molecular hyperpolarizability elements. The hyperpolarizability elements of an α -helix can be obtained from the product of the components of the Raman polarizability and IR transition dipole moment.

Due to the limited resolution of many SFG spectrometers ($\sim 5 \text{ cm}^{-1}$ or more), the A mode and E_1 mode cannot be readily resolved in the frequency domain, and therefore, the total susceptibility is often assumed to be the sum of the susceptibilities from these two modes:⁷

$$\chi_{yyz} = \chi_{A,yyz} + \chi_{E_1,yyz} \quad (\text{S10})$$

$$\chi_{zzz} = \chi_{A,zzz} + \chi_{E_1,zzz} \quad (\text{S11})$$

According to equations (S4)-(S11), the orientation angle (θ) can be obtained by measuring the ppp and ssp spectral intensity ratio of peptide amide I signals (eqs. S12 and 13).

$$\chi_{ssp} = F_{ssp} N_s \left[\left(\frac{1+r}{2} - \frac{\beta_{aca}}{\beta_{ccc}} \right) \langle \cos \theta \rangle - \left(\frac{1-r}{2} - \frac{\beta_{aca}}{\beta_{ccc}} \right) \langle \cos^3 \theta \rangle \right] \beta_{ccc} \quad (\text{S12})$$

$$\chi_{ppp} = F_{ppp} N_s \left[\left(r + \frac{2\beta_{aca}}{\beta_{ccc}} \right) \langle \cos \theta \rangle + \left(1-r - \frac{2\beta_{aca}}{\beta_{ccc}} \right) \langle \cos^3 \theta \rangle \right] \beta_{ccc} \quad (\text{S13})$$

The change of the number of alamethicin inserted into the bilayer due to the pH change is then given by equation S14 or S15:

$$\frac{N_s^{pH2}}{N_s^{pH1}} = \frac{\chi_{ssp}^{pH2} \left[\left(\frac{1+r}{2} - \frac{\beta_{aca}}{\beta_{ccc}} \right) \langle \cos \theta_{pH1} \rangle - \left(\frac{1-r}{2} - \frac{\beta_{aca}}{\beta_{ccc}} \right) \langle \cos^3 \theta_{pH1} \rangle \right]}{\chi_{ssp}^{pH1} \left[\left(\frac{1+r}{2} - \frac{\beta_{aca}}{\beta_{ccc}} \right) \langle \cos \theta_{pH2} \rangle - \left(\frac{1-r}{2} - \frac{\beta_{aca}}{\beta_{ccc}} \right) \langle \cos^3 \theta_{pH2} \rangle \right]} \quad (\text{S14})$$

$$\frac{N_s^{pH2}}{N_s^{pH1}} = \frac{\chi_{ppp}^{pH2} \left[\left(r + \frac{2\beta_{aca}}{\beta_{ccc}} \right) \langle \cos \theta_{pH1} \rangle + \left(1-r - \frac{2\beta_{aca}}{\beta_{ccc}} \right) \langle \cos^3 \theta_{pH1} \rangle \right]}{\chi_{ppp}^{pH1} \left[\left(r + \frac{2\beta_{aca}}{\beta_{ccc}} \right) \langle \cos \theta_{pH2} \rangle + \left(1-r - \frac{2\beta_{aca}}{\beta_{ccc}} \right) \langle \cos^3 \theta_{pH2} \rangle \right]} \quad (\text{S15})$$

In order to calculate the orientation angle for a 3_{10} helix in a lipid membrane, we developed the orientation analysis method similar to that used for alpha helices.⁹ We deduced the relation between the χ_{ppp}/χ_{ssp} value and the 3_{10} -helix orientation with a δ - or Gaussian distribution using different hyperpolarizability tensor elements with the adoption of the bond additivity model. Thus the orientation angle (θ) of a 3_{10} helix as well as an alpha helix can be deduced by measuring the ppp and ssp spectral intensity ratio of peptide amide I signal, as shown in Figure S2 and S3.

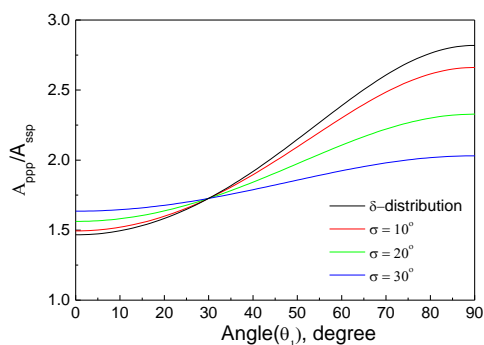


Figure S2. The relation between SFG susceptibility tensor component ratio for the helix containing 1-13 residues and the helix orientation angle (where $r = 0.6547$; $\beta_{aca}/\beta_{ccc} = 0.3595$ in eqs. S6-S9).

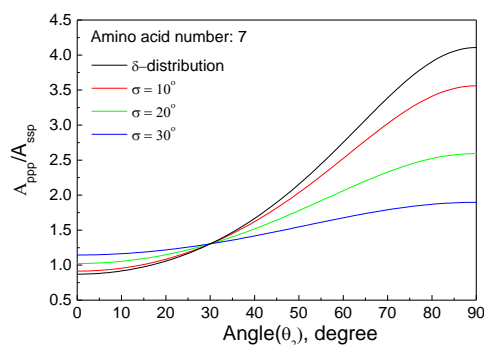


Figure S3. The relation between SFG susceptibility tensor component ratio and the 3_{10} -helix orientation angle. (where $r = 1.102$; $\beta_{aca}/\beta_{ccc} = 0.5407$ in eqs. S6-S9).

5. Fitting parameters and the fitting errors of SFG spectra

Table S1. Fitting parameters for SFG spectra shown in Figure 1 and Figure 3

		pH = 6.7			pH = 11.9		
		ssp	ppp	$\frac{(A/\Gamma)_{ppp}}{(A/\Gamma)_{ssp}}$	ssp	ppp	$\frac{(A/\Gamma)_{ppp}}{(A/\Gamma)_{ssp}}$
χ_{NR}		-2.39	-3.1		-13.4	-28.8	
Peak 1	A	43.8(2.7)	95.5(4.5)		125.6(10.4)	243.0(10.7)	1.93
	$\omega(\text{cm}^{-1})$	1638	1638	2.18	1638	1638	
	$\Gamma(\text{cm}^{-1})$	9.0	9.0		9.0	9.0	
Peak 2	A	242.4(5.3)	642.4(12.4)	2.65	995.3(27.7)	2329.7(90)	2.34
	$\omega(\text{cm}^{-1})$	1671	1671		1671	1671	
	$\Gamma(\text{cm}^{-1})$	18.0	18.0		18.0	18.0	
Peak 3	A	32.1 (12.6)	48.5(9.3)	2.39	-409.2(59.7)	-1285(98)	3.10
	$\omega(\text{cm}^{-1})$	1720.7	1710.6		1580	1580	
	$\Gamma(\text{cm}^{-1})$	10.6	6.7		50.0	50.0	

The fitting errors are included in parentheses.

6. The effect of salt

We investigated the effect of salt on the SFG signals from alamethicin in a POPC/POPC bilayer at pH=6.7. After adding 300 μ L KCl solution (1M) (pH=6.7) into the aqueous subphase (resulting in a 0.16M KCl solution), alamethicin amide I intensity decreased (Figure S4).

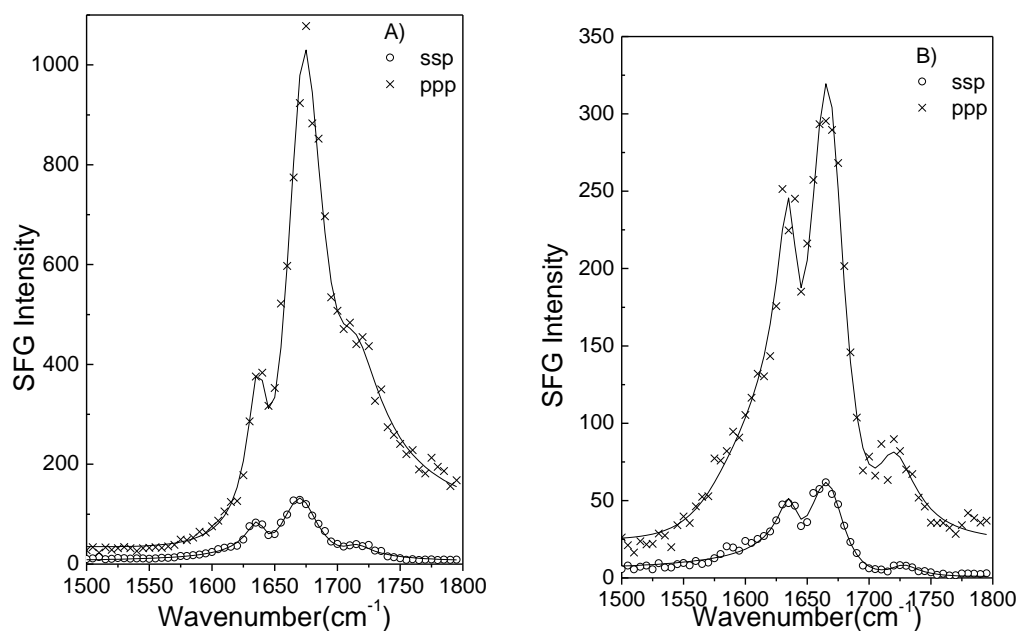


Figure S4: SFG spectra collected from alamethicin in a POPC/POPC bilayer in contact with alamethicin solution of pH=6.7. A) before and B) after the addition of KCl to the subphase.

7. No apparent secondary structural changes for alamethicin at different pH

We performed unpolarized ATR-FTIR measurements and Circular Dichroism (CD) experiments on alamethicin associated with POPC/POPC lipids at different pH values to show that no apparent secondary structural change for alamethicin occurred at different pH, 6.7 vs. 11.9.

7.1 Unpolarized ATR-FTIR experiments: Figure S5 shows the unpolarized ATR-FTIR spectra collected from the POPC/POPC bilayer in contact with (a) alamethicin solution with a pH of 6.7, (b) alamethicin solution with a pH of 11.9, and (c) sample (a) after raising the subphase pH to 11.9. For comparison purposes, all spectra were normalized to

a constant intensity. Clearly, the spectra are quite similar, showing that no apparent secondary structural change of alamethicin in the lipid bilayer was detected when the subphase pH was varied (6.7 vs. 11.9). This is reasonable because the ATR-FTIR signals were generated from the peptides in the lipid bilayer. The interactions between the lipids and the peptides should be more or less similar, regardless of subphase pH.

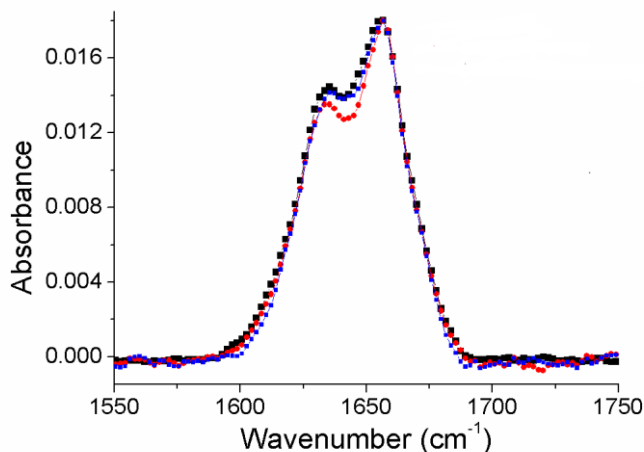


Figure S5: Unpolarized ATR-FTIR spectra collected from the POPC/POPC bilayer in contact with (a) alamethicin solution with a pH of 6.7 (black), (b) alamethicin solution with a pH of 11.9 (blue), and (c) sample (a) after raising the subphase pH to 11.9 (red).

7.2 CD measurements We also collected CD spectra from alamethicin in POPC lipid vesicle solutions at pH 6.7 and 11.9.

Vesicle Preparation: Lipid solutions of POPC dissolved in chloroform were purchased from Avanti Polar Lipids, Inc. Lipids were dried under a continuous stream of nitrogen gas for 2+ hrs to remove the solvent, and the dried lipids were reconstituted in Millipore water to a final concentration of 2 mg/mL of the desired lipid of choice. This solution was allowed to sit for two hours at room temperature while continuously agitated using a vortex mixer at medium speed. Vesicles were prepared via extrusion through 50 nm pore size filters.

CD Experiments: Prior to the first sample run, a 1mm pathlength spectrosil cuvette was cleaned by soaking in 1M nitric acid for 20min, followed by several rinses with water and methanol. The cuvette was thoroughly dried under a stream of N₂. Due to time and

equipment limitations, the full cleaning procedure could not be used in between samples collected on the same day. Following the first sample, the cuvette was rinsed thoroughly 4x with Millipore water, then dried with methanol under nitrogen. A CD spectrum was then collected from the blank cuvette filled with Millipore water to ensure that no residual protein or phosphate signals could be observed, after which time the water was removed and replaced with the appropriate sample.

All CD spectra were collected using an Aviv 202 spectrometer with a temperature controlled cell at 25° C. Multiple spectra were collected in the range 190-260 nm, with a 2-4 second averaging time per datapoint. Spectra of the peptide in vesicles were also compared to the peptide in water (not shown) to confirm that the signals obtained were for peptides in a lipid environment. In these experiments, the vesicle and stock solutions were mixed together and diluted to a final concentration of ~60µM peptide and ~1200µM lipid, for a final lipid/peptide ratio of 20:1. To ensure good stirring, these samples were vortex mixed in a small centrifuge tube for 60 sec before being added to the sample cuvette.

Due to unfavorable absorption of UV light at lower wavelengths by phosphate ions, spectra at pH 11.9 are also collected using NaOH to control the pH, and the results were comparable to those determined using K₃PO₄.

Figure S6 shows that the CD spectra collected from alamethicin in POPC vesicle solutions at different pH values are identical, indicating no secondary structural change for alamethicin.

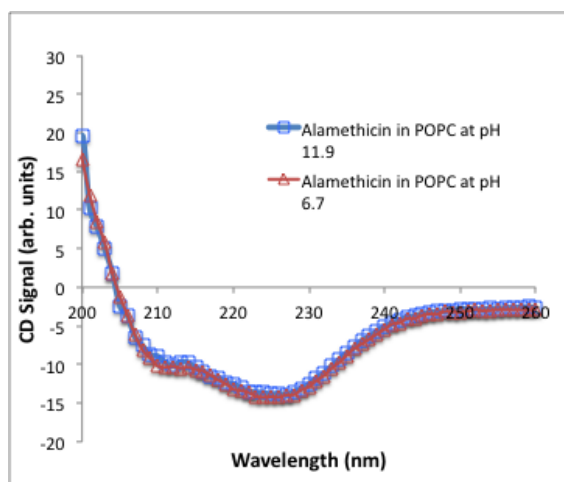


Figure S6: CD spectra collected from alamethicin in POPC vesicle solutions at pH 6.7 and 11.9.

8. Reversibility of pH effects in SFG experiments

After the spectra in Figure 3 were collected, we brought the pH back to ~ 7 by adding H_3PO_4 (in 1M stock solution) to the subphase. About $40\mu\text{L}$ H_3PO_4 (1M) solution was injected into the subphase and then SFG spectra were collected after the equilibrium (the pH of the subphase is about 8.0). After that, an additional $20\mu\text{L}$ H_3PO_4 (1M) solution was injected into the subphase and SFG spectra were collected again after equilibrium (the pH of the subphase was measured to be ~ 7.0). With the addition of H_3PO_4 , the SFG intensity decreases quickly (Figures S7 and S8).

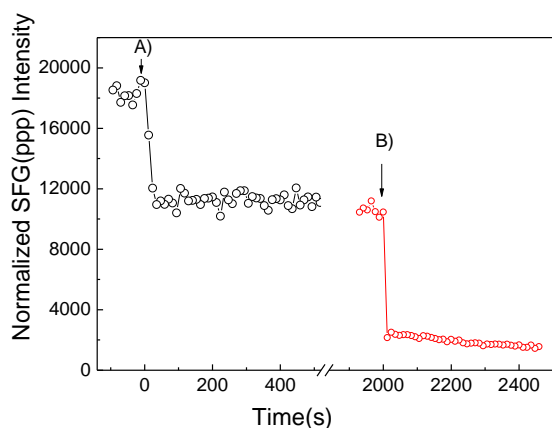


Figure S7. The time-dependent intensity change of ppp SFG spectra at 1665 cm^{-1} in the alamethicin associated with the POPC/POPC bilayer. A) After the spectra in Figure 3 were collected, about $40\mu\text{L}$ H_3PO_4 (in 1M stock solution) was injected at time A; B) additional $20\mu\text{L}$ H_3PO_4 (in 1M stock solution) was added at time B).

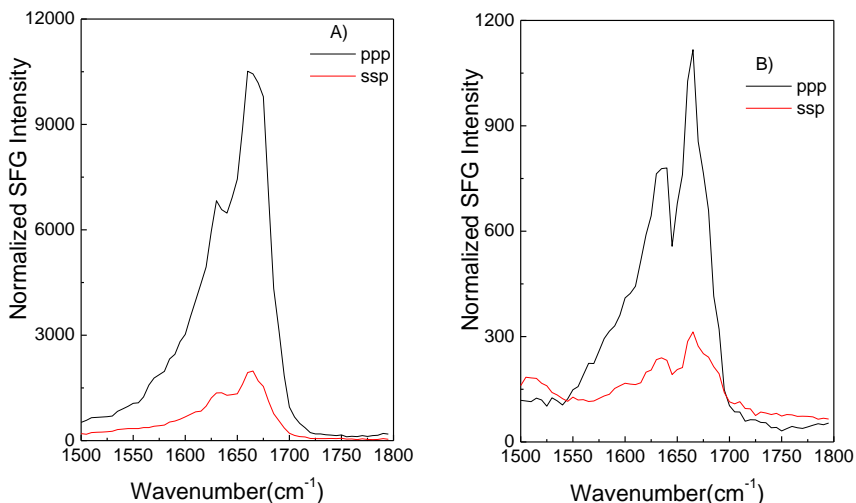


Figure S8. A) After the SFG spectra in Figure 3 were collected, about 40 μL $\text{H}_3\text{PO}_4(1\text{M})$ was injected into the subphase and SFG spectra were collected after equilibration; B) After spectra in panel A were collected, additional 20 μL $\text{H}_3\text{PO}_4(1\text{M})$ was injected into the subphase and SFG spectra were collected after equilibration.

9. Fluorescence measurements

Extensive studies have suggested that membrane potentials can be measured directly using fluorescence spectroscopy.¹²⁻¹⁵ The membrane surface potential can be calculated according to the Nernst equation,¹²⁻¹⁶

$$\Psi = -(pK_{ch} - pK_0) \times \frac{2.303RT}{F} \quad (\text{S16})$$

where pK_{ch} and pK_0 denote the apparent dissociation constants of the fluorescent dye at a charged and a neutral interface, respectively; ψ is the membrane potential; R is the gas constant; T is the temperature in degree Kelvin, and F is Faraday's constant. pK_{ch} and pK_0 can be obtained by measuring the dependence of the dye's degree of dissociation (α) upon the pH of the aqueous bulk medium (pH), and calculated according to

$$pK = pH - \log\left[\frac{\alpha}{1-\alpha}\right] \quad (\text{S17})$$

Two different bilayers (10% Rhod-DMPE+90%POPC)/POPC (dye in inner leaflet) and POPC/(10% Rhod-DMPE+90%POPC) (dye in outer leaflet) were prepared on right-angle CaF_2 prisms using the same LB/LS methods discussed previously. The

fluorescence signals from these bilayers and a monolayer of (10%Rhod-DMPE+90%POPC) on water surface were collected using our SFG system and experimental geometry. The visible beam of 532 nm was used as the excitation source. The IR beam was blocked when scanning the fluorescence signal from 540 nm to 650 nm. The fluorescence spectra at pH =7.3 and pH = 11.8 are shown in Figure S9.

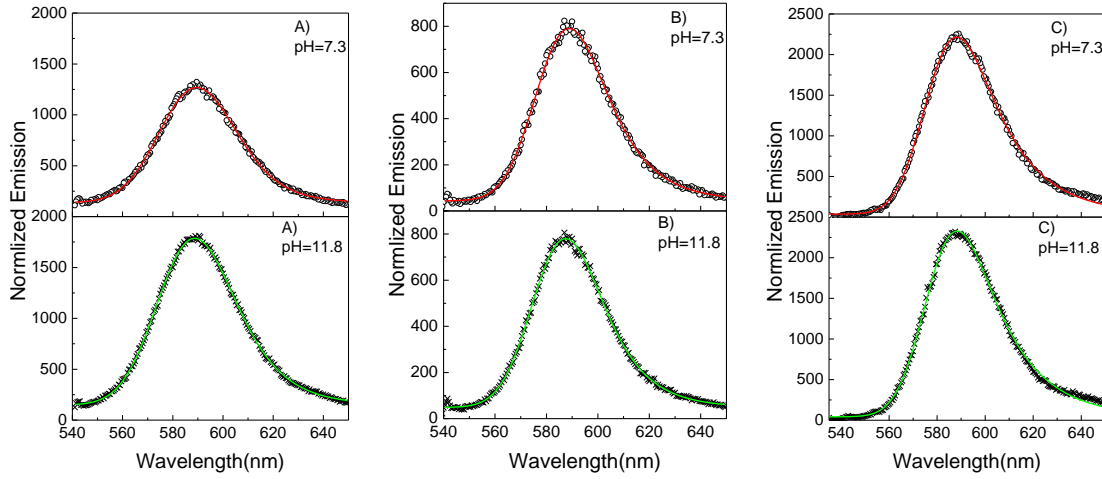


Figure S9. Fluorescence spectra. A) bilayer of (10%Rhod-DMPE+90%POPC) /POPC; B) bilayer of POPC/(10%Rhod-DMPE+90%POPC); C) monolayer of (10%Rhod-DMPE+90%POPC) on water surface.

When the incident angle of the excitation beam on the sample interface is greater than the critical angle, the laser can create an exponentially decaying evanescent field that selectively excites fluorophores within several hundred nanometers from the surface. An exponentially modified Gaussian function has been frequently used to fit fluorescence emission spectra,¹⁷⁻¹⁹ and will be used in our fitting as shown in equation S18.

$$f(x) = y_0 + \frac{A}{t_0} e^{\frac{1}{2}(\frac{w}{t_0})^2 \frac{x-x_c}{t_0}} \int_{-\infty}^z \frac{1}{\sqrt{2\pi}} e^{-\frac{y^2}{2}} dy \quad (\text{S18})$$

where $z = \frac{x-x_c}{w} - \frac{w}{t_0}$; y_0 , A , x_c , w and t_0 represent the offset, peak area, peak center, peak width and time constant of exponential axis, respectively. The fitting results are present in Table S2.

Table S2. The fitting parameters for the fluorescence spectra shown in Figure S4.

membrane	pH	Fitting Parameters				
		y_0	A	x_c	w	t_0
Bilayer A)	7.3	254.1	75603	581.3	14.55	11.55
Bilayer A)	11.8	46.0	142017	577.5	11.85	22.51
Bilayer B)	7.3	43.8	28280	580.1	11.00	13.74
Bilayer B)	11.8	48.5	27240	579.0	11.12	12.86
Monolayer C)	7.3	30.7	97237	579.0	10.38	19.86
Monolayer C)	11.8	30.1	97325	578.7	10.64	17.89

When the pH increased from 7.3 to 11.8, the fluorescence intensity (peak area) from the bilayer (10%Rhod-DMPE+90%POPC)/POPC increased 1.88 times while the intensity changes from the bilayer of POPC/(10%Rhod-DMPE+90%POPC) and monolayer (10%Rhod-DMPE+90%POPC) were negligible. Since the dissociation constant α is proportional to the measured fluorescence intensity,¹²⁻¹⁶ the membrane potential difference can be calculated according to equations S4-S5, assuming $\alpha \ll 1$.

$$\Psi_{pH=7.3} = \frac{-2.303RT}{F} \log \frac{I_{out}^{7.3}}{I_{inner}^{7.3}} \quad (S19)$$

$$\Psi_{pH=11.8} = \frac{-2.303RT}{F} \log \frac{I_{out}^{11.8}}{I_{inner}^{11.8}} \quad (S20)$$

I_{out} and I_{inner} are the fluorescence intensity from the outer leaflet and inner leaflet of the bilayer. When the pH value was changed from 7.3 to 11.8, the potential difference ($\Delta\Psi = \Psi_{pH=11.8} - \Psi_{pH=7.3}$) of POPC/POPC bilayer is then estimated to be -16.2 mV. This value agrees with the results of phospholipid 1-stearoyl-2-oleoyl-phosphatidyl-choline reported by Zhou et al.²⁰

References

1. Wang, J.; Chen, C. Y.; Buck, S. M.; Chen, Z. *J. Phys. Chem. B* **2001**, *105*, 12118–12125.
2. Tamm, L. K.; Tatulian, U. A. *Quart. Rev. Biophys.* **1997**, *30*, 365-429.
3. Kass, I.; Arbey, E.; Arkin, I. T. *Biophys. J.* **2004**, *86*, 2502-2507.
4. Marsh, D.; Muller, M.; Schmitt, F. -J. *Biophys. J.* **2000**, *78*, 2499-2510.
5. Malcolm, B. R.; Walkinshaw, M. D. *Biopolymers* **1986**, *25*, 607-625.
6. Y. R. Shen, *The Principles of Nonlinear Optics*; John Wiley & Sons: New York, 1984.
7. Chen, X.; Wang, J.; Boughton, A. P.; Kristalyn, C. B.; Chen, Z. *J. Am. Chem. Soc.* **2007**, *129*, 1420-1427.
8. Wang, J.; Lee, S. H.; Chen, Z. *J. Phys. Chem. B* **2008**, *112*, 2281-2290.
9. Nguyen, K. T.; Le Clair, S.; Ye, S.J.; Chen, Z. *J. Phys. Chem. B* **2009**, *113*, 12169–12180.
10. Lee, S.; Wang, J.; Krimm, S.; Chen, Z. *J. Phys. Chem. A* **2006**, *110*, 7035-7044.
11. Ye, S. J.; Nguyen, K. T.; Le Clair, S.; Chen, Z. *J. Struct. Biol.* **2009**, *168*, 61-77.
12. Shapiro, H.M. *Methods* **2000**, *21*, 271-279.
13. Cohen, L.B.; Salzberg, B.M. *Rev. Physiol. Biochem. Pharmacol.* **1978**, *83*, 35-88.
14. Plfigek, J.; Sigler, K. *J. Photochem. Photobio. B* **1996**, *33*, 101-124.
15. Starke-Peterkovic, T.; Clarke, R.J. *Eur. Biophys. J.* **2009**, *39*, 103–110.
16. Schummer, U.; Schiefer, H.G. *Febs Lett.* **1988**, *236*, 337-339.
17. Heider, E.C.; Barhoum, M.; Peterson, E.M.; Jschaefel, J.; Harris, J.M. *Appl. Spect.* **2010**, *64*, 37-45.
18. Fox, C.B.; Wayment, J.R.; Myers, G.A.; Endicott, S.K. Harris, J.M. *Anal. Chem.* **2009**, *81*, 5130–5138.
19. Tylli, H.; Forsskahl, I.; Olkkonen, C. *J. Photochem. Photobio. A* **1995**, *87*, 181-191.
20. Zhou, Y.; Raphael, R.M. *Biophys. J.* **2007**, *92*, 2451–2462.